Breakthrough Technologies

Activity Profiling of Papain-Like Cysteine Proteases in Plants[1]

Renier A. L. van der Hoorn*, Michiel A. Leeuwenburgh, Matthew Bogyo, Matthieu H. A. J. Joosten, and Scott C. Peck

Laboratory of Phytopathology, Wageningen University, 6709 PD, Wageningen, The Netherlands (R.A.L.v.d.H., M.H.A.J.J.); Sainsbury Laboratory, John Innes Centre, NR4–7UH, Norwich, United Kingdom (R.A.L.v.d.H., S.C.P.); Leiden Institute of Chemistry, Gorlaeus Laboratories, Leiden University, 2300 RA, Leiden, The Netherlands (M.A.L.); and Department of Pathology, Stanford University Medical School, Stanford, California 94305–5324 (M.B.)

Transcriptomic and proteomic technologies are generating a wealth of data that are frequently used by scientists to predict the function of proteins based on their expression or presence. However, activity of many proteins, such as transcription factors, kinases, and proteases, depends on posttranslational modifications that frequently are not detected by these technologies. Therefore, to monitor activity of proteases rather than their abundance, we introduce protease activity profiling in plants. This technology is based on the use of biotinylated, irreversible protease inhibitors that react with active proteases in a mechanism-based manner. Using a biotinylated derivative of the Cys protease inhibitor E-64, we display simultaneous activities of many papain-like Cys proteases in extracts from various tissues and from different plant species. Labeling is pH dependent, stimulated with reducing agents, and inhibited specifically by Cys protease inhibitors but not by inhibitors of other protease classes. Using one-step affinity capture of biotinylated proteases followed by sequencing mass spectrometry, we identified proteases that include xylem-specific XCP2, desiccation-induced RD21, and cathepsin B- and aleurain-like proteases. Together, these results demonstrate that this technology can identify differentially activated proteases and/or characterize the activity of a particular protease within complex mixtures.

Plant genomes encode hundreds of proteases, but little is known about what roles they play in the life of a plant. Functions for only a few of the more than 550 proteases of Arabidopsis (http://merops.sanger.ac.uk) have been determined genetically (for review, see Adam and Clarke, 2002; Beers et al., 2004). In general, proteases are thought to be involved in a range of processes, including senescence and defense responses (Beers et al., 2000; Van der Hoorn and Jones, 2004), as indicated by studies with protease inhibitors (e.g. Solomon et al., 1999; Chichkova et al., 2004). In many cases, proposed functions for proteases have been inferred from the observed differential expression of their mRNAs (e.g. Zhao et al., 2000; Gepstein et al., 2003). The progress in assigning roles for proteases, however, is significantly impeded by their redundancy and posttranslational regulation.

Typically, proteases contain an autoinhibitory prodomain that must be removed to activate the enzyme (Bryan, 2002). The activity of many proteases also depends on pH, indicative of the compartment where they localize and on the presence of endogenous pro-tease inhibitors or activators (Beynon and Bond, 2000). Activities of many proteases have been shown using zymograms or chromogenic substrates (Michaud, 1998), but these approaches require at least partial purification of the protease to discriminate it from other protease activities. Recently, a novel technology became available that deals with problems associated with redundancy and posttranslational activation. This technology, called protease activity profiling, displays activities rather than abundance of proteases and can be used to simultaneously demonstrate activities of multiple proteases of particular catalytic classes (for review, see Campbell and Szardenings, 2003).

Proteases are classified based on their catalytic mechanisms into Ser, Cys, aspartic, and metallo proteases (Powers et al., 2002). All four classes, usually distinguished by their active site residues, are represented in the Arabidopsis genome. The Ser proteases comprise the largest class with approximately 200 members, and the Cys, aspartic, and metallo protease classes each contain about 100 members (http://merops.sanger.ac.uk; Van der Hoorn and Jones, 2004). Among the largest protease families in Arabidopsis are subtilisin-like Ser proteases (58 members in family S8 of clan SB) and papain-like Cys proteases (30 members in family C1 of clan CA; Beers et al., 2004). Within these families, most proteases are produced as pre-pro-proteases with a signal sequence, an autoinhibitory prodomain, and a similarly sized mature protease domain.

To cleave a peptide bond, Ser and Cys proteases contain a Ser or Cys residue, respectively, in their active site that acts as a nucleophile in the first step of proteolysis (Powers et al., 2002). This nucleophilic attack results in an intermediate state where the enzyme is covalently attached to the substrate. Subsequent hydrolysis results in cleavage of the peptide bond and release of the protease (Powers et al., 2002). Many class-specific inhibitors of Ser and Cys proteases act as suicide substrates, locking the cleavage mechanism in the covalent intermediate state. Examples of these irreversible, mechanism-based inhibitors are di-isopropyl fluorophosphate (DFP) for Ser proteases and E-64 for Cys proteases of the CA clan (Powers et al., 2002).

Protease activity profiling is based on biotinylated (or otherwise labeled) mechanism-based protease inhibitors that covalently react with proteases in an activity-dependent manner (Campbell and Szardenings, 2003). Activities of most Ser proteases can be profiled using FP-biotin, a biotinylated derivative of (DFP) (Liu et al., 1999), whereas papain-like Cys proteases can be profiled with DCG-04, a biotinylated derivative of E-64 (Greenbaum et al., 2000; Fig. 1A). Biotinylated proteases can be quantified by immunoblot analysis using streptavidine-peroxidase conjugates or purified on immobilized streptavidin for identification by mass spectrometry (Fig. 1B).

The simultaneous visualization of multiple protease activities will become an essential tool to unravel functions of the hundreds of proteases encoded by plant genomes. To date, however, protease activity profiling has only been used with mammalian and Drosophila proteases (Jessani et al., 2002; Kocks et al., 2003). In this study, we show that protease activity profiling can also be applied on plant extracts. After establishing parameters for labeling, we identified activities of different Cys proteases in a whole-plant extract and show an example where induction of a protease gene during senescence is not correlated with the activity of the encoded enzyme. Our data demonstrate the versatility of the technology and indicate that its application will provide important data on activities of many plant proteases.

RESULTS

Optimization of Protease Activity Profiling on Arabidopsis Leaf Extracts

To establish protease activity profiling in plants, we optimized a protocol for profiling protease activities in extracts of Arabidopsis leaves (Fig. 1C, and "Material and Methods"). Labeling Arabidopsis leaf extracts typically results in signals in three major regions: 40, 30, and 25 kD (Fig. 1C, indicated with black, white, and gray dots, respectively). Each of these signals was competed with an excess of E-64, indicating specific labeling. Although only three prominent signals are visible, protein blots of higher resolution indicated
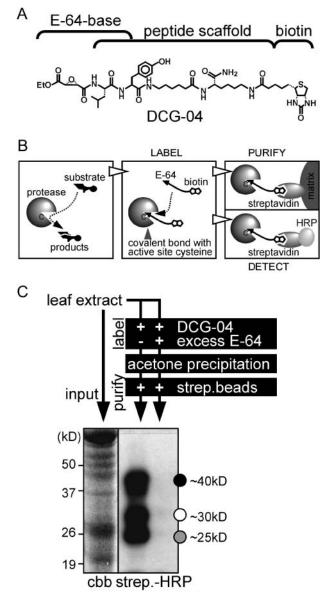

Figure 1. Mechanism and procedure of protease activity profiling in plants. A, Structure of DCG-04, a biotinylated derivative of the E-64 Cys protease inhibitor. B, Mechanism of Cys protease activity profiling. An active Cys protease (left) cleaves protein substrates through a covalent intermediate state, mediated by the catalytic Cys (C) in the active site. Biotinylation of active proteases (middle) by DCG-04 occurs because the cleavage mechanism is locked in the covalent intermediate state. The biotinylated protease can be purified on immobilized streptavidin (right, top) or detected on a protein gel blot using a conjugate of streptavidin with HRP (right, bottom). C, Experimental procedure for protease activity profiling. A total protein extract is labeled by adding DCG-04. To determine the specificity of labeling, in the control experiment an excess of E-64 is added (for details, see "Materials and Methods"). Labeling buffer and excess DCG-04 are removed by acetone precipitation. Biotinylated proteins are purified on streptavidin beads to enhance the signal and reduce background signals, separated on a SDS protein gel, and subsequently transferred to a membrane and detected with streptavidin-HRP and chemiluminescence. Input proteins are visualized on a Coomassie (cbb)-stained protein gel. When applied to Arabidopsis leaf extracts, this procedure typically results in three major signals of 40, 30, and 25 kD (indicated with black, white, and gray dots, respectively).

that the upper and lower signals are composed of multiple bands (see later, e.g. Figs. 2 and 6), indicating that multiple active proteases of similar sizes are visualized.

Numerous parameters needed to be optimized for sensitive and reproducible labeling. Usually, about 0.7 mg of soluble protein was taken for each profiling reaction (one leaf half). However, dilution experiments showed that the same signals could be detected with 100-fold less input proteins, demonstrating the sensitivity of the procedure (data not shown). Specific labeling was detected within 5 min incubation (Fig. 2A, left), but a maximum was reached after 5 h labeling (Fig. 2A, right). Optimal labeling also required the presence of reducing agents (Fig. 2B). This observation is explained by inactivation of Cys proteases by oxidation of the active site Cys during protein extraction (Beynon and Bond, 2000). Finally, labeling was usually performed at pH 6, but when labeling was done at different pH values, profiles changed significantly (Fig. 2C). This result indicates that the choice of pH is crucial for the types of proteases that are intended to be displayed. The changes in relative intensities at different pH also indicate that different proteases are displayed, rather than one with different molecular masses. For all subsequent experiments, we chose the optimum labeling conditions, meaning high concentrations of soluble protein and 5 h labeling time at pH 6 in the presence of the reducing agent L-Cys.

Inhibition of Labeling by Protease Inhibitors

To confirm that the signals on the protein blots represent Cys proteases, labeling was performed in the presence of other inhibitors of Cys proteases (cystatin, antipain, leupeptin, and chymostatin) and inhibitors of Ser proteases (phenylmethylsulfonyl fluoride [PMSF]), metallo proteases (EDTA), and aspartic proteases (pepstatin). These experiments show that labeling is inhibited by other Cys protease inhibitors (Fig. 3A) but not by inhibitors of proteases from the other classes (Fig. 3B). The slightly reduced labeling at high PMSF concentrations is because PMSF also inhibits Cys proteases at high concentrations (Beynon and Bond, 2000). The inhibition profiles are not the same for all Cys protease inhibitors. The 25-kD signals, for example, are more efficiently inhibited by antipain than by the other Cys protease inhibitors (Fig. 3A). This result again indicates that the signals represent different Cys proteases, rather than one with different molecular masses.
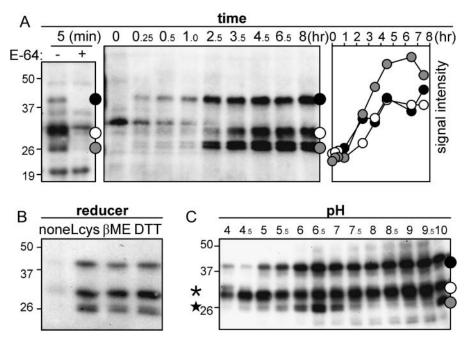

Figure 2. Optimization of protease labeling. A, Time course of labeling of active Cys proteases. Arabidopsis leaf extract was labeled at room temperature, at pH 6. Samples were taken at various time points, and the presence of biotinylated proteins was analyzed as described in Figure 1C. Specific protease signals (indicated with dots on the right) start to appear within 5 min (left). The additional signals in the left panel result from longer exposure and are background signals since they are not competed with E-64. The intensities of the bands present in the middle panel were measured and plotted against time (right). Maximal labeling is reached after about 5 h. B, Labeling requires reducing agents. Labeling of leaf extract at pH 6 for 5 h was done in the absence of reducer (none) or in the presence of L-Cys (Lcys; 2 mg mL^{-1}), β-mercaptoethanol (βME; 1% v/v), or dithiotreitol (DTT; 2 mg mL^{-1}). Biotinylated proteins were analyzed as described in Figure 1C. C, pH dependency of labeling. Leaf extracts were labeled for 5 h at various pH values. Proteases indicated with a star and asterisk show optimum labeling at neutral and acidic pH, respectively. Biotinylated proteins were analyzed as described in Figure 1C.
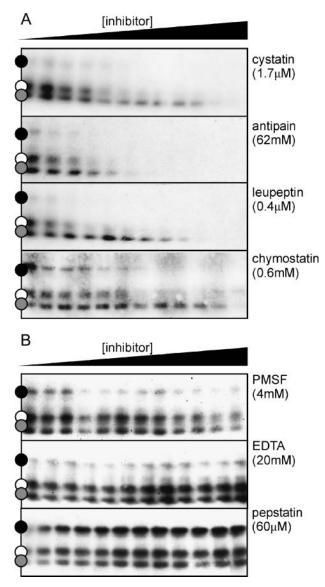
Figure 3. Inhibition of protease labeling by protease inhibitors. Labeling of leaf proteases (pH 6, for 5 h) was done in the presence of an increasing amount of inhibitors of Cys proteases (A), or Ser (PMSF), metallo (EDTA), and aspartic (pepstatin) proteases (B). The highest inhibitor concentration that was used (in the right-most lane) is indicated between brackets. These concentrations were step-wise diluted 3-fold, from right to left. Biotinylated proteins were analyzed as described in Figure 1C.

Protease Activity Profiles of Other Organs of Arabidopsis

Having established labeling conditions of leaf extracts, we examined protease activity profiles of other Arabidopsis organs. Interestingly, although all signals still occur at the 25-, 30-, and 40-kD regions, the profiles differ significantly in molecular masses and in their relative intensities (Fig. 4). The profile obtained from a flower extract even displayed nine bands, illustrating that different tissues express unique patterns of protease activities.

Purification and Identification of Biotinylated Cys Proteases

A large-scale labeling and purification was performed to identify the different biotinylated proteases. An extract from nine plants was labeled at pH 6, proteins were precipitated by acetone, and biotinylated proteases were purified on immobilized streptavidin. To monitor the purification procedure, samples were taken at each step. We noticed that much of the 40-kD signal was lost after dissolving the acetone pellet, apparently because these proteins do not redissolve well (Fig. 5A).

Biotinylated proteins isolated from the soluble extract were analyzed on a streptavidin-horseradish peroxidase (HRP)-stained protein blot and on a colloidal Coomassie-stained protein gel (Fig. 5B). Only four bands appeared on the protein gel, and each band was competed with an excess of E-64 during labeling (Fig. 5B, right). These signals matched the major biotinylated signals (Fig. 5B, left). The four bands were excised from the protein gel, and after in-gel digestion with trypsin, the resulting tryptic fragments were analyzed by matrix-assisted laser-desorption ionization time of flight (MALDI-TOF)-mass spectrometry (MS) and quadrupole (Q)-TOF-MS/MS.

In total, six different Cys proteases were identified unambiguously (Table I; Fig. 5C). Three of the four bands contained multiple proteases, and two proteases were identified twice, in bands 1 and 2 (Table I; Fig. 6C). Three of the proteases, Arabidopsis aleurain-like protease (AALP; Ahmed et al., 2000), xylem-specific Cys protease-2 (XCP2; Zhao et al., 2000), and the drought-induced RD21 protease (Koizumi et al., 1993), have been described previously. The three
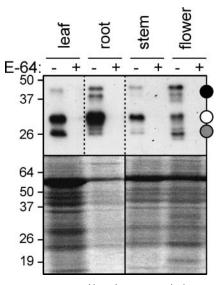

Figure 4. Protease activity profiles of various Arabidopsis organs. Total extracts from leaf (one leaf), root (of nine plants), stem (10 cm), and flower (20 flowers) were subjected to standard protease activity profiling (pH 6, 5 h labeling). The Coomassie-stained protein gel in the bottom panel shows the total amount of input proteins.
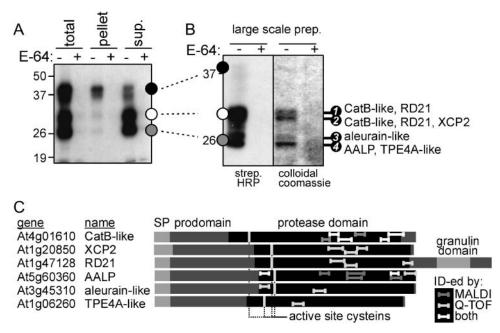
Figure 5. Large-scale purification and identification of biotinylated Cys proteases. A, Total extract of 6-week-old Arabidopsis plants (nine plants) was labeled with DCG-04 (5 h labeling at pH 6). Small-scale samples were taken to monitor the purification procedure. This revealed that proteases at 40 kD are difficult to redissolve after acetone precipitation. B, Analysis of large-scale purified biotinylated proteins. Biotinylated proteins were purified from the supernatant of the large-scale labeling and analyzed with streptavidin-HRP (left) and colloidal Coomassie stain (right). Stained bands (numbered 1–4) were excised and analyzed by MALDI-MS and Q-TOF-MS/MS. Identified proteases for each band are indicated on the right. C, Protein structures of the identified proteases. All protease domains are preceded by a signal peptide (SP) and a prodomain. Only RD21 also carries a C-terminal extension, containing a granulin domain. Tryptic fragments identified by MALDI-MS, Q-TOF-MS/MS, or both are indicated in the proteins with dark gray, light gray, and white bars, respectively.

additional proteases that were identified show homology to a tobacco cathepsin B-like protease (Lidgett et al., 1995), barley aleurain (Rogers et al., 1985), and pea TPE4A (Cercos et al., 1999). These new proteins are named CatB-like, aleurain-like, and TPE4A-like proteases, respectively. To our knowledge, the intrinsic activities of these proteases have not been previously demonstrated.

All six protease genes are predicted to encode proteins containing a signal peptide, a prodomain, and the protease domain (Fig. 5C). Only RD21 has an additional C-terminal extension containing a granulin domain (Yamada et al., 2001). The identified tryptic fragments were derived only from the protease domain and not the prodomain (Fig. 5C), consistent with the inhibitory role of the prodomain that needs to be removed before the protease can react with DCG-04. Tryptic fragments carrying the active site Cys (Fig. 5C) were not identified, most likely because biotinylation of these fragments by DCG-04 yields peptides that are too large to be detected.

Confirmation of the Identity of the Cys Proteases with Specific Antibodies

Of the identified Cys proteases, specific antibodies have been raised to XCP2 (E. Beers and E. Petzold, unpublished data), AALP (Ahmed et al., 2000), and

RD21 (Yamada et al., 2001). To confirm that these proteases are indeed proteins that become biotinylated, we labeled a leaf extract with DCG-04 and isolated biotinylated proteins using immobilized streptavidin. Subsequently, the biotinylated proteins were analyzed on protein blots with the protease-specific antibodies. For each of these proteases, a signal of the expected size was detected among the biotinylated proteins. Thus, anti-XCP2, anti-AALP, and anti-RD21 show E-64-competable signals in the 30-, 25-, and 30-kD regions, respectively (Fig. 6A), from which these proteins were identified (Fig. 5B). Thus, XCP2, AALP, and RD21 are indeed among the biotinylated, active proteases.

Intriguingly, the anti-RD21 antibody also cross-reacts with biotinylated proteins in the 40-kD region (Fig. 6A). This observation is consistent with previous studies. RD21 is known to exist in two active forms, a 38-kD intermediate form (iRD21) containing the C-terminal granulin domain, and a 33-kD mature form (mRD21) from which the granulin domain has been removed (Yamada et al., 2001). The iRD21 tends to aggregate, probably caused by the C-terminal granulin domain (Yamada et al., 2001). Therefore, the proteins in the 40-kD region, from which we could not identify proteases as they precipitated during large-scale purification, may contain the 38-kD iRD21. Indeed, when the precipitate of the large-scale purifi-

Table I. *Identified sequences of Cys proteases of Arabidopsis*

Gene[a]	Name[b]	Overall Score[c]	Peptide Sequences[d]	Parent Molecular Mass[e]	Protein Band[f]	Individual Score[g]
At4g01610	CatB-like	162 (No. 1); 178 (No. 2)	GWGDDGYFMIR	1,315.58	1	40
			GWGDDGYFMIR	1,315.58	2	53
			GWGDDGYFM^{ox}IR	1,331.56	2	48
			SNPQDIMAEVYK	1,393.65	1	42
			SNPQDIMAEVYK	1,393.69	2	69
			SNPQDIM^{ox}AEVYK	1,409.65	1	60
			SNPQDIM^{ox}AEVYK	1,409.65	2	60
			GTNECGIEDEPVAGLPSSK	1,958.90	1	62
			NGPVEVSFTVYEDFAHYK	2,100.97	2	55
At1g20850	XCP2	144	EFQFYSGGVFDGR	1,507.68	2	60
			ALAHQPLSVAIDASGR	1,604.86	2	43
			DESETVTINGHQDVPTNDEK	2,227.00	2	42
At1g47128	RD21	93 (No. 1); 175 (No. 2)	CGIAIEPSYPIK	1,346.68	1	93
			CGIAIEPSYPIK	1,346.69	2	74
			AVAHQPISIAIEAGGR	1,588.87	2	34
			VVTIDSYEDVPTYSEESLK	2,173.04	2	66
At5g60360	AALP	74	DWREDGIVSPVK	1,399.71	4	31
			NSWGADWGDK	1,134.48	4	22
			NMCGIATCASYPVVA	1,628.71	4	22
At3g45310	Aleurain-like	89	DWREDGIVSPVK	1,399.70	3	36
			YNGGLDTEEAYPYTGK	1,776.79	3	53
At1g06260	TPE4A-like	59	GCSGGLM^{ox}ETAFEFIK	1,661.75	4	59

[a]Arabidopsis gene locus name. [b]Given name. [c]Overall MOWSE score for identified protein (No. indicates the protein band of Fig. 5B). [d]Sequence determined by Q-TOF (M^{ox}, oxidized Met). [e]Observed molecular mass of parent peptide. [f]Protein band of Figure 5B, from which the peptide has been identified. [g]MOWSE score for determined sequence, given by Mascot.

cation was analyzed with anti-RD21 antibody, a clear signal indicates that iRD21 is present (Fig. 6B).

The AALP and RD21 transcripts have been shown to accumulate during leaf senescence (Gepstein et al., 2003). To test whether the corresponding activity of these proteases also increases, we performed protease activity profiling on mature and senescing leaves and analyzed biotinylated proteins with anti-AALP and anti-RD21 antibodies. Protease activity profiling showed a general increase in Cys protease activity in
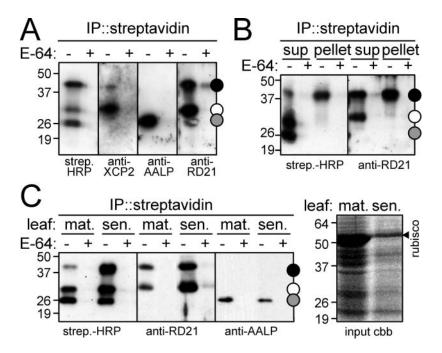

Figure 6. Confirmation of the identity of the isolated proteases with protease-specific antibodies. A, Biotinylated proteases from leaves were purified and analyzed with streptavidin-HRP or antibodies against XCP2, AALP, and RD21. These antibodies indicate specific labeling of the corresponding proteases at sizes predicted by their initial identification (Fig. 5B). Note that a second, 40-kD signal cross-reacts with the RD21 antibody. B, Undissolved biotinylated proteins contain the 40 kD form of RD21. Biotinylated proteases present in supernatant and pellet after dissolving the acetone pellet were purified and analyzed with streptavidin-HRP and RD21 antibody. Note that the pellet shows a clear 40-kD band in both cases. C, Activity of RD21 and AALP in senescing leaves. Proteases of mature (mat.) and senescing (sen.) leaves were biotinylated, purified, and analyzed by streptavidin-HRP, anti-RD21, or anti-AALP antibody (left). The right panel shows input proteins, separated on a Coomassie (cbb)-stained protein gel. Note that the RD21 activity increases, whereas the AALP activity appears to decrease in senescing leaves.

senescing leaves (Fig. 6C, left), particularly when the lower protein concentrations used for these samples are considered (Fig. 6C, right). Consistent with the results predicted by the increased transcript abundance, a significantly higher level of active RD21 was present in extracts of senescing leaves (Fig. 6C). By contrast, the activity of AALP was unchanged, if not slightly lower in extracts of senescing leaves (Fig. 6C). These results provide a clear illustration of the fact that the activity of proteases may not be correlated with mRNA or protein levels.

Protease Activity Profiling in Other (Model) Plant Species

In principle, Cys protease activity profiling can be performed on any tissue containing Cys proteases that are inhibited by E-64. To demonstrate its wider applicability, we performed protease activity profiling on leaf extracts of various model plant species. The resulting protease activity profiles are highly polymorphic, with molecular masses ranging from 25 to 40 kD (Fig. 7), indicating that different Cys proteases are labeled in different plant species. Thus, this method can be applied in a broad spectrum of plant species.

DISCUSSION

Here, we have shown that protease activity profiling can be used to monitor protease activities in plant tissues. We have identified six different Cys proteases form Arabidopsis, three of which were known only from the genome sequence. To our knowledge, for all proteases, including those previously described (XCP2, AALP, and RD21), activity had not been demonstrated. An essential feature of the technology is that it detects the activity of proteases because E-64 acts as a suicide substrate, locking the cleavage mechanism in the covalent intermediate state. Indeed, labeling is pH dependent, can be stimulated with reducing agents, and is inhibited by Cys protease inhibitors but not by inhibitors of other catalytic classes, all of which are characteristics that typify the activity of Cys proteases (Beynon and Bond, 2000). In addition, as expected for the broad specificity for the E-64-based probe, the six proteases that we identified in this study represent five of the eight groups that have been distinguished within 30 members of Arabidopsis papain-like proteases (Beers et al., 2004).

Protease activity profiling has two primary applications. One is to search for differentially activated proteases in a particular biological system, as we showed for different Arabidopsis organs (Fig. 4). The procedure to separate the different biotinylated proteases, however, may still need to be optimized to deal with the overlapping complexity, for example using two-dimensional gel electrophoresis or multidimensional liquid chromatography-mass spectrometry. The other application is to use protease activity profiling when a particular enzyme is under investigation. Combined with protease-specific antibodies, protease activity profiling can be used to study the activity of a particular protease without the need to purify it from its native environment. For example, we examined activities of RD21 and AALP in extracts of senescing tissues (Fig. 6C). A similar procedure can be used to determine the optimum pH for the activity of a certain protease or to screen for inhibitors and determine a relative inhibition constant.

A number of variations can be exploited to gain additional information from protease activity profiling. First, conditions for protease labeling can be chosen (e.g. pH), offering opportunities to display subsets of protease activities. Second, protease activity profiling can be performed not only with total extracts of plants but also with subproteomes, such as proteins from the extracellular space, membranes, or isolated organelles. This approach may reveal low-abundant protease activities and also reduce the chances of accidentally activated proteases that may result from cellular disruption. Third, use of probes different from DCG-04 (used in this study) can reveal activities of other proteases. There are probes with a broad specificity described for Ser proteases (Liu et al., 1999), and deubuiqitinating enzymes (Borodovsky et al., 2001), whereas many other probes for other proteases are under development (Campbell and Szardenings, 2003).

Finally, it must be acknowledged that the activity detected in extracts may not reflect the in planta acti-
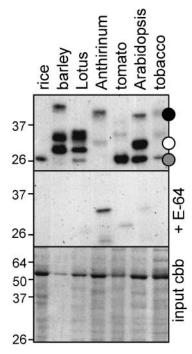

Figure 7. Protease activity profiling in other (model) plant species. Cys proteases in extracts of leaf tissues (from 1 cm² each) were biotinylated, purified, and analyzed with streptavidine-HRP. The bottom panel shows the input proteins, separated on a Coomassie (cbb)-stained protein gel.

vity in all cases. Detected activities may change as a result of extraction, where normally compartmentalized proteases are mixed, possibly leading to activation. This problem could be circumvented by including inhibitors of other protease classes and by using subproteomes. With the development of membrane-permeable probes, it may even be possible to bring the probe into living systems without disrupting the cellular structure.

The proteases identified in this study are of unknown function, but their proposed roles can be of great interest. XCP2, for example, is hypothesized to be involved in programmed cell death of tracheary elements (Funk et al., 2002). Furthermore, RD21 is present in endoplasmic reticulum (ER) bodies that originate from the ER and fuse with the vacuole upon stress (Hayashi et al., 2001). These ER bodies are wound inducible and are thought to be part of an herbivore-defense mechanism (Hara-Nishimura and Matsushima, 2003). In addition, the CatB-like protease belongs to a group of senescence-induced proteases that also includes AALP and RD21 (Bhalerao et al., 2003; Gepstein et al., 2003). These senescence-induced proteases likely play a role in (regulation of) protein degradation as part of programmed cell death. Thus, although little is known about the role of these and other proteases, we can now begin to study their individual activities and to define their function.

MATERIALS AND METHODS

Plant Materials, Reagents, and Antibodies

Arabidopsis ecotype Columbia was grown in a growth chamber at 22°C under 16-h light regime. Tissues were taken from 6-week-old plants that just started flowering. Model plant species were grown in a normal greenhouse.

DCG-04 was synthesized and purified as described previously (Greenbaum et al., 2000). E-64, cystatin, antipain, leupeptin, chymostatin, PMSF, and pepstatin were purchased from Sigma (Dorset, UK).

Antibodies for detection of XCP2, AALP, and RD21 were kindly provided by Dr. Eric Beers and Dr. Earl Petzold, Dr. Natasha Raikhel, and Dr. Ikuko Hara-Nishimura, respectively. Anti-rabbit IgG antibodies, conjugated with HRP, are from Amersham Pharmacia Biotech (Bucks, UK).

Protease Activity Profiling

Proteins were extracted by grinding one rosette leaf in an Eppendorf tube, mixing with 0.5 mL of water, and centrifugation through a micro Biospin column (Bio-Rad, Hercules, CA). Usually, approximately 0.5 mg of protein was labeled in 0.5 mL of total volume, containing 50 mM sodium acetate buffer, pH 6, 10 mM L-Cys (Sigma), and 2 μM DCG-04. Control samples contained also 0.2 mM E-64. Labeling was done for 5 h at room temperature.

Proteins were then precipitated by adding 1 mL ice-cold acetone, followed by centrifugation (1 min, 10,000g). The acetone pellet was washed with 70% acetone and dissolved in 500 μL of TBS (50 mM Tris, pH 7.5, 150 mM NaCl) containing a protease inhibitor cocktail (Complete tablet; Roche, Mannheim, Germany) and 10 μL of TBS-washed magnetic streptavidin beads (Promega, Southampton, UK). Solutions with streptavidin beads were gently shaken overnight at room temperature. The beads were then washed once with TBS using a magnetic holder and boiled in 50 μL of SDS sample buffer. More extensive washes with TBS were done for detection with protease-specific antibodies.

Biotinylated proteins were separated on 10% SDS gels (Laemmli, 1970), transferred onto polyvinylidene fluoride membrane (PVDF, Bio-Rad), and

detected with streptavidin-HRP (1:3,000, Ultrasensitive, Sigma) or protease-specific antibodies (1:1,000) and anti-rabbit-HRP (1:3,000).

A time course of labeling was done by taking aliquots from a large-scale labeling and stopping the labeling by adding an excess of E-64 followed by acetone precipitation. Profiling at different pH was done using 50 mM buffers of sodium acetate (pH 4–6.5) or Tris (pH 7–10). Competition of protease labeling by protease inhibitors was done by preincubating the extracts at pH 6 for 10 min with 3-fold dilution series of various protease inhibitors.

Large-Scale Profiling and Identification of Cys Proteases

Large-scale purification was done similarly as above and is detailed below. Complete 6-week-old plants (nine individuals) were ground with sand and water in a mortar. The extract was centrifuged (15 min, 10,000g), and the supernatant was taken for labeling. Labeling was done for 6 h at 19°C in 45 mL total volume containing 50 mM sodium acetate buffer, pH 6; 0.4 mM PMSF, 10 mM EDTA; 10 mM L-Cys; and 0.2 mM DCG-04 (and 10 mM E-64 only in the control). Proteins were precipitated with 90 mL of cold acetone, and the pellet was washed with 70% acetone. Proteins were dissolved from the acetone pellet into 45 mL of TBS and centrifuged to remove nondissolved precipitate. Before and after this centrifugation, samples were taken for small-scale purification as described above. Protease inhibitor cocktail and 100 μL of TBS-washed magnetic streptavidin beads were added to the supernatant. After overnight incubation at room temperature, streptavidin beads were collected in an Eppendorf tube using a magnetic holder and washed twice with TBS; twice with TBS containing 1 M NaCl; twice with TBS containing 1% Triton X-100; and once with water, and then boiled in 50 μL of SDS sample buffer. Proteins present in 3 μL of sample were separated on a large 10% SDS gel and transferred to polyvinylidene difluoride for detection with streptavidin-HRP, whereas the remainder of the sample was separated on the same large SDS-gel for staining with colloidal Coomassie Brilliant Blue.

Bands were excised from the Coomassie-stained gel and subjected to in-gel tryptic digestion (Shevchenko et al., 1996). Tryptic peptides were eluted and analyzed by MALDI-TOF-MS and Q-TOF-MS/MS (John Innes Centre Proteomics Facility, Norwich, UK). Data were analyzed with Mascot and MS-Fit from Protein Prospector (http://prospector.ucsf.edu/) and subjected to database searches against the National Center for Biotechnology Information nonredundant database.

Sequence data from this article have been deposited with the EMBL/GenBank data libraries under accession numbers At4g01610 (CatB-like), At1g20850 (XCP2), At1g47128 (RD21), At5g60360 (AALP), At3g45310 (aleurain-like), and At1g06260 (TPE4A-like).

LITERATURE CITED

Adam Z, Clarke AK (2002) Cutting edge of chloroplast proteolysis. Trends Plant Sci **7:** 451–456

Ahmed SU, Rojo E, Kovaleva V, Venkataraman S, Dombrowski JE, Matsuoka K, Raikhel NV (2000) The plant vacuolar sorting receptor AtELP is involved in transport of NH₂-terminal propeptide-containing vacuolar proteins in *Arabidopsis thaliana.* J Cell Biol **149:** 1335–1344

Beers EP, Jones AM, Dickerman AW (2004) The S8 serine, C1A cysteine and A1 aspartic protease families in Arabidopsis. Phytochemistry **65:** 43–58

Beers EP, Woffenden BJ, Zhao C (2000) Plant proteolytic enzymes: possible roles during programmed cell death. Plant Mol Biol **44:** 399–415

Beynon R, Bond JS (2000) Proteolytic Enzymes, Ed 2, Series Practical Approach. Oxford University Press, Oxford

Bhalerao R, Keskitalo J, Sterky F, Erlandsson R, Bjorkbacka H, Birve SJ,

Karlsson J, Gardestrom P, Lundeberg J, Jansson S (2003) Gene expression in autumn leaves. Plant Physiol **131:** 430–442

Borodovsky A, Kessler BM, Casagrande R, Overkleeft HS, Wilkinson KD, Ploegh HL (2001) A novel active site-directed probe specific for deubiquitylating enzymes reveals proteasome association of USP14. EMBO J **20:** 5187–5196

Bryan PN (2002) Prodomains and protein folding catalysis. Chem Rev **102:** 4805–4815

Campbell DA, Szardenings AK (2003) Functional profiling the proteome with affinity labels. Curr Opin Chem Biol **7:** 296–303

Cercos M, Santamaria S, Carbonell J (1999) Cloning and characterisation of TPE4A, a thiol-protease gene induced during ovary senescence and seed germination in pea. Plant Physiol **119:** 1341–1348

Chichkova NV, Kim SH, Titova ES, Kalkum M, Morozov VS, Rubtsov YP, Kalinina NO, Taliansky ME, Vartapetian AB (2004) A plant caspase-like protease activated during the hypersensitive response. Plant Cell **16:** 157–171

Funk V, Kositsup B, Zhao C, Beers EP (2002) The Arabidopsis xylem peptidase XCP1 is a tracheary element vacuolar protein that may be a papain ortholog. Plant Physiol **128:** 84–94

Gepstein S, Sabehi G, Carp M-J, Hajouj T, Nesher MF, Yariv I, Dor C, Bassani M (2003) Large-scale identification of leaf senescence-associated genes. Plant J **36:** 629–642

Greenbaum D, Medzihradszky KF, Burlingame A, Bogyo M (2000) Epoxide electrophiles as activity-dependent cysteine protease profiling and discovery tools. Chem Biol **7:** 569–581

Hara-Nishimura I, Matsushima R (2003) A wound-inducible organelle derived from the endoplasmic reticulum: a plant strategy against environmental stresses? Curr Opin Plant Biol **6:** 583–588

Hayashi Y, Yamada K, Shimada T, Matsushima R, Nishizawa NK, Nishimura M, Hara-Nishimura I (2001) A proteinase-storing body that prepares for cell death or stresses in the epidermal cells of Arabidopsis. Plant Cell Physiol **42:** 894–899

Jessani N, Liu Y, Humphrey M, Cravatt BF (2002) Enzyme activity profiles of the secreted and membrane proteome that depict cancer cell invasiveness. Proc Natl Acad Sci USA **99:** 10335–10340

Kocks C, Maehr R, Overkleeft HS, Wang EW, Iyer LK, Lennon-Dumeni A-M, Ploegh HL, Kessler BM (2003) Functional proteomics of the active cysteine protease content in Drosophila S2 cells. Mol Cell Proteomics **2:** 1188–1197

Koizumi M, Yamaguchi-Shinozaki K, Tsuji H, Shinozaki K (1993) Structure and expression of two genes that encode distinct drought-inducible cysteine proteinases in *Arabidopsis thaliana.* Gene **129:** 175–182

Laemmli UK (1970) Cleavage of structural proteins during the assembly of the head of bacteriophage T4. Nature **227:** 680–685

Lidgett AJ, Moran M, Wong KA, Furze J, Rhodes MJ, Hamill D (1995) Isolation and expression pattern of a cDNA encoding a cathepsin B-like protease from *Nicotiana rustica.* Plant Mol Biol **29:** 379–384

Liu Y, Patricelli MP, Cravatt BF (1999) Activity-based protein profiling: the serine hydrolases. Proc Natl Acad Sci USA **96:** 14694–14699

Michaud D (1998) Gel electrophoresis of proteolytic enzymes. Anal Chim Acta **372:** 173–185

Powers JC, Asgian JL, Ekici OD, James KE (2002) Irreversible inhibitors of serine, cysteine, and threonine proteases. Chem Rev **102:** 4639–4750

Rogers JC, Dean D, Heck GR (1985) Aleurain: a barley thiol protease closely related to mammalian cathepsin H. Proc Natl Acad Sci USA **82:** 6512–6516

Shevchenko A, Jensen ON, Podtelejnikov AV, Sagliocco F, Wilm M, Vorm O, Mortensen P, Shevchenko A, Boucherie H, Mann M (1996) Linking genome and proteome by mass spectrometry: large-scale identification of yeast proteins from two dimensional gels. Proc Natl Acad Sci USA **93:** 14440–14445

Solomon M, Belenghi B, Delledonne M, Menachem E, Levine A (1999) The involvement of cysteine proteases and protease inhibitor genes in the regulation of programmed cell death in plants. Plant Cell **11:** 431–443

Van der Hoorn RAL, Jones JDG (2004) The plant proteolytic machinery and its role in defence. Curr Opin Plant Biol (in press)

Yamada K, Matsushima R, Nishimura M, Hara-Nishimura I (2001) A slow maturation of a cysteine protease with a granulin domain in the vacuoles of senescing Arabidopsis leaves. Plant Physiol **127:** 1626–1634

Zhao C, Johnson BJ, Kositsup B, Beers EP (2000) Exploiting secondary growth in Arabidopsis. Construction of xylem and bark cDNA libraries and cloning of three xylem endopeptidases. Plant Physiol **123:** 1185–1196